Molecular Dynamics Simulations of Polyelectrolyte Adsorption

Jan-Michael Y. Carrillo and Andrey V. Dobrynin*

Polymer Program, Institute of Materials Science and Department of Physics, University of Connecticut, Storrs, Connecticut 06269

Received October 19, 2006

We have performed molecular dynamics simulations of polyelectrolyte adsorption at oppositely charged surfaces from dilute polyelectrolyte solutions. In our simulations, polyelectrolytes were modeled by chains of charged Lennard-Jones particles with explicit counterions. We have studied the effects of the surface charge density, surface charge distribution, solvent quality for the polymer backbone, strength of the short-range interactions between polymers and substrates on the polymer surface coverage, and the thickness of the adsorbed layer. The polymer surface coverage monotonically increases with increasing surface charge density for almost all studied systems except for the system of hydrophilic polyelectrolytes adsorbing at hydrophilic surfaces. In this case the polymer surface coverage saturates at high surface charge densities. This is due to additional monomer−monomer repulsion between adsorbed polymer chains, which becomes important in dense polymeric layers. These interactions also preclude surface overcharging by hydrophilic polyelectrolytes at high surface charge densities. The thickness of the adsorbed layer shows monotonic dependence on the surface charge density for the systems of hydrophobic polyelectrolytes for both hydrophobic and hydrophilic surfaces. Thickness is a decreasing function of the surface charge density in the case of hydrophilic surfaces while it increases with the surface charge density for hydrophobic substrates. Qualitatively different behavior is observed for the thickness of the adsorbed layer of hydrophilic polyelectrolytes at hydrophilic surfaces. In this case, thickness first decreases with increasing surface charge density, then it begins to increase.

1. Introduction

Adsorption of charged polymers at surfaces and interfaces plays an important role in different areas of natural sciences including materials science,[1−3] colloidal science,[4,5] and biophysics.[6,7] For example, polyelectrolyte adsorption found its application for colloidal stabilization and flocculation.[4,5] It is utilized for assembly of multicomponent nanocomposite films by the successive deposition of positively and negatively charged macromolecules on charged surfaces from aqueous solutions.[3,8−12] The adsorption of the DNA and RNA molecules onto the interior of the viral capcid provides the driving force for viral self-assembly and storage of the genetic material.[13] Adsorption of proteins and DNA onto cell membranes is the initial step in the macromolecule uptake into the cell interior.[14]

Over the last 40 years the adsorption of charged polymers has been under extensive theoretical,[15−36] computational,[37−45] and experimental[46−62] studies. It was established that the polyelectrolyte adsorption depends strongly on the key parameters of the systems such as surface charge density, fraction of charged monomers on the polymer backbone, polymer−solvent and polymer−surface affinity, and pH and ionic strength of the solutions. The combined effect of these factors can lead to a

(1) Wagberg, L. *Nord. Pulp Pap. Res. J.* **2000**, *15*, 586−597.
(2) Fleer, G. J.; Cohen Stuart, M. A.; Scheutjens, J. M. H. M.; Gasgove, T.; Vincent, B. *Polymer at interfaces*; Chapman and Hall: London, 1993.
(3) *Multilayer Thin Films*; Decher, G., Schlenhoff, J. B., Eds.; Wiley-VCH: Weinheim, 2003.
(4) Dubin, P.; Bock, J.; Davis, R.; Schulz, D. N.; Thies, C. *Macromolecular Complexes in Chemistry and Biology*; Springer-Verlag: Berlin, 1994.
(5) Dubin, P. L.; Farinato, R. S. *Colloid−Polymer Interactions: From Fundamentals to Practice*; Wiley-Interscience: New York, 1999.
(6) Levin, Y. *Rep. Prog. Phys.* **2002**, *65*, 1577−1632.
(7) Grosberg, A. Y.; Nguyen, T. T.; Shklovskii, B. I. *Rev. Mod. Phys.* **2002**, *74*, 329−345.
(8) Sukhishvili, S. A. *Curr. Opin. Colloid Interface Sci.* **2005**, *10*, 37−44.
(9) Schonhoff, M. *Curr. Opin. Colloid Interface Sci.* **2003**, *8*, 86−95.
(10) Kotov N. A. *Multilayer Thin Films*; Wiley-VCH: Weinheim, 2003; Chapter 8, pp 207−244.
(11) Rubner M. F. *Multilayer Thin Films*; Wiley-VCH: Weinheim, 2003; Chapter 5, pp 133−154.
(12) Sukhorukov, G. B.; Fery, A.; Mohwald, H. *Prog. Polym. Sci.* **2005**, *30*, 885−897.
(13) van der Schoot, P.; Bruinsma, R. *Phys. Rev. E* **2005**, *71*, 061928-1-12.
(14) Mathews, C. K.; Van Holde, K. E.; Ahern, K. G. *Biochemistry*; Benjamin/Cummings: San Francisco, CA, 2000.
(15) Shafir, A.; Andelman, D. *Phys. Rev. E* **2004**, *70*, 061804-1-12.
(16) Cheng, H.; De La Cruz, M. O. *J. Polym. Sci., Part B: Polym. Phys.* **2004**, *42*, 3642−3653.
(17) Cheng, H.; De La Cruz, M. O. *J. Chem. Phys.* **2003**, *119*, 12635−12644.
(18) Dobrynin, A. V.; Deshkovski, A.; Rubinstein, M. *Phys. Rev. Lett.* **2000**, *84*, 3101−3104.
(19) Joanny, J. F. *Eur. Phys. J. B* **1999**, *9*, 117−122.
(20) Stuart, M. A. C.; Hoogendam, C. W.; deKeizer, A. *J. Phys.: Condens. Matter* **1997**, *9*, 7767−7783.
(21) Netz, R. R.; Joanny, J. F. *Macromolecules* **1999**, *32*, 9013−9025.
(22) Chatellier, X.; Joanny, J. F. *J. Phys. II* **1996**, *6*, 1669−1686.
(23) Dobrynin, A. V.; Deshkovski, A.; Rubinstein, M. *Macromolecules* **2001**, *34*, 3421−3436.
(24) Borisov, O. V.; Zhulina, E. B.; Birshtein, T. M. *J. Phys. II* **1994**, *4*, 913−929.
(25) Muthukumar, M. *J. Chem. Phys.* **1987**, *86*, 7230−7235.
(26) van der Schee, H. A.; Lyklema, J. *J. Phys. Chem.* **1984**, *88*, 6661−6672.
(27) Borisov, O. V.; Hakem, F.; Vilgis, T. A.; Joanny, J. F.; Johner, A. *Eur. Phys. J. E* **2001**, *6*, 37−47.
(28) Wang, Q.; Taniguchi, T.; Fredrickson, G. H. *J. Phys. Chem. B* **2004**, *108*, 6733−6744.
(29) Dobrynin, A. V.; Rubinstein, M. *J. Phys. Chem. B* **2003**, *107*, 8260−8269.
(30) Cheng, C.-H.; Lai, P.-Y. *Phys. Rev. E* **2004**, *70*, 061805-1-4.
(31) Dobrynin, A. V. *J. Chem. Phys.* **2001**, *114*, 8145−8153.
(32) Dobrynin, A. V.; Rubinstein, M. *Macromolecules* **2002**, *35*, 2754−2768.
(33) Wang, Q. *J. Phys. Chem. B* **2006**, *110*, 5825−5828.
(34) Shafir, A.; Andelman, D. *Eur. Phys. J. E* **2006**, *19*, 155−162.
(35) Patra, C. N.; Chang, R.; Yethiraj, A. *J. Phys. Chem. B* **2004**, *108*, 9126−9132.
(36) Winkler, R. G.; Cherstvy, A. G. *Phys. Rev. Lett.* **2006**, *96*, 066103-1-4.
(37) Dias, R. S.; Pais, A. A. C. C.; Linse, P.; Miguel, M. G.; Lindman, B. *J. Phys. Chem. B* **2005**, *109*, 11781−11788.
(38) Laguecir, A.; Stoll, S. *Polymer* **2005**, *46*, 1359−1372.
(39) Stoll, S.; Chodanowski, P. *Macromolecules* **2002**, *35*, 9556−9562.
(40) Yamakov, V.; Milchev, A.; Borisov, O.; Dunweg, B. *J. Phys.: Condens. Matter* **1999**, *11*, 9907−9923.
(41) Patel, P. A.; Jeon, J.; Mather, P. T.; Dobrynin, A. V. *Langmuir* **2005**, *21*, 6113−6122.
(42) Panchagnula, V.; Jeon, J.; Dobrynin, A. V. *Phys. Rev. Lett.* **2004**, *93*, 037801−1.−4.
(43) Messina, R. *Phys. Rev. E* **2004**, *70*, 051802-1-9.
(44) Abu-Sharkh, B. *J. Chem. Phys.* **2005**, *123*, 114907-1-6.
(45) Reddy, G.; Chang, R.; Yethiraj, A. *J. Chem. Theory Comput.* **2006**, *2*, 630−636.

10.1021/la063079f CCC: $37.00
Published on Web 01/30/2007

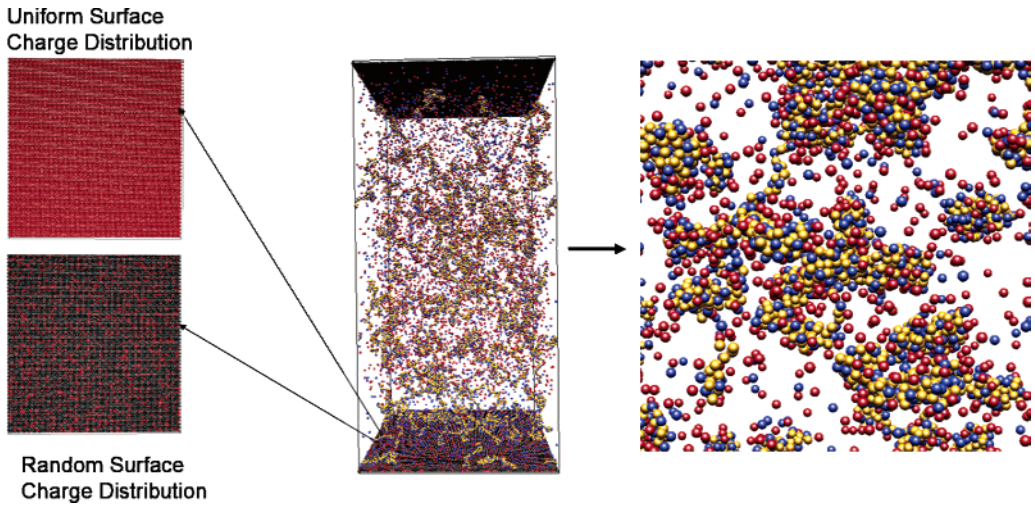

Figure 1. Snapshot of the simulation box filled with polyelectrolytes and counterions. The charged surface is located at the bottom of the simulation box and a neutral surface is placed at the top of the box. The system is periodic in *x* and *y* directions. The charged surface has either random or uniform charge distribution (see inset on the left). Neutral monomers are colored in yellow, negatively charged monomers and surface counterions are shown in blue, positively charged counterions and positively charged surface beads are colored in red, and neutral beads on the surface are shown in black.

peculiar behavior of the adsorbed polymers. Depending on the fraction of charged monomers on the polymer backbone and polymer affinity to the adsorbing surface, a polymer surface coverage can increase[51,52,55,56] or decrease[48,53,54,63] with increasing salt concentration. In some cases, the polymer adsorbed amount varies nonmonotonically and exhibits a maximum as a function of the solution ionic strength.[49] This complicated ionic strength dependence of the polymer surface coverage is a result of a fine interplay between long-range electrostatic and short-range interactions between polymers and substrate.

Adsorbed polyelectrolyte chains could be trapped in metastable states due to strong electrostatic interactions with a charged substrate.[47,64] It was observed that polystyrene sulfonate adsorbed on a ferric oxide from solution with low ionic strengths cannot be displaced by chains with higher molecular weight, indicating existence of a higher potential barrier precluding a chain desorption. The studies of the chain exchange kinetics between poly(1,4-vinylpyridine) polymers with different degrees of ionization adsorbed at silicon oxide showed long-lived metastable states with lifetime longer than 2−3 days. The chain's exchange rate increases, and metastability completely disappears with increasing solution ionic strength. The salt dependence of the exchange rate points to the electrostatic nature of the metastable states. The reported values of the adsorption energy of charged units are of the order of 4−7 k_BT, where k_B is the Boltzmann constant and T is the absolute temperature.

Table 1. System Sizes Used in Simulations

	N_p, 61				
Σ (σ^{-2})	Z_{box} (σ)	N_{mon}	N_s	$N_c^{\pm}$	N_{tot}
0.072	161.4	2684	3840	1044	7568
0.144	161.4	2684	3840	1164	7688
0.231	165.1	2745	3840	1329	7914
0.289	172.4	2867	3840	1467	8174
0.385	231.1	3843	3840	1963	9646
0.462	278.8	4636	3840	2364	10840
0.577	344.8	5734	3840	2934	12508

Theoretical studies of polyelectrolyte adsorption were focused on a single chain adsorption−desorption transition at charged surface,[24,25,27,30] charged cylinder,[65] and charged sphere;[36,39,66,67] on the effect of the surface charge density and polymer surface affinity on conformations of a weakly charged polyelectrolyte chain near a charged surface;[24,68] on the dependence of the thickness of the adsorbed layer, polymer surface coverage on the solution ionic strength, and pH; and on the solvent quality for the polymer backbone and the strength of the short-range polymer surface interactions.[18,20−23,26,28−34,69] The theoretical models of polyelectrolyte adsorption were also used to calculate the effective interactions between charged surfaces.[70−72]

Recent theoretical developments in the area of polyelectrolyte adsorption (for recent review see ref 73) were stimulated by the

(46) Shulga, A.; Widmaier, J.; Pefferkorn, E.; Champ, S.; Auweter, H. *J. Colloid Interface Sci.* **2003**, *258*, 219−227.
(47) Mubarekyan, E.; Santore, M. *Macromolecules* **2001**, *34*, 7504−7513.
(48) Shubin, V.; Linse, P. *J. Phys. Chem.* **1995**, *99*, 1285−1291.
(49) Van de Steeg, H. G. M.; deKeizer, A.; Stuart, M. A. C.; Bijsterbosch, B. H. *Colloids Surf., A* **1993**, *70*, 77−89.
(50) Van de Steeg, H. G. M.; Stuart, M. A. C.; deKeizer, A.; Bijsterbosch, B. H. *Langmuir* **1992**, *8*, 2538−2546.
(51) Popping, B.; Deratani, A.; Sebille, B.; Desbois, N.; Lamarche, J. M.; Foissy, A. *Colloids Surf.* **1992**, *64*, 125−133.
(52) Papenhuijzen, J.; Fleer, G. J.; Bijsterbosch, B. H. *J. Colloid Interface Sci.* **1985**, *104*, 553−561.
(53) Durand-Piana, G.; Lafuma, F.; Audebert, R. *J. Colloid Interface Sci.* **1987**, *119*, 474−480.
(54) Hendrickson, E.; Neuman, R. D. *J. Colloid Interface Sci.* **1986**, *110*, 243−251.
(55) Kawaguchi, M.; Takahashi, A. *Adv. Colloid Interface Sci.* **1992**, *37*, 219−317.
(56) Marra, J.; van der Schee, H. A.; Fleer, G. J.; Lyklema, J. In *Adsorption in Solutions*.
(57) Kawaguchi, M.; Kawaguchi, H.; Takahashi, A. *J. Colloid Interface Sci.* **1988**, *124*, 57−62.
(58) Plunkett, M. A.; Claesson, P. M.; Ernstsson, M.; Rutland, M. W. *Langmuir* **2003**, *19*, 4673−4681.
(59) Vagharchakian, L.; Desbat, B.; Henon, S. *Macromolecules* **2004**, *37*, 8715−8720.
(60) Abu-Sharkh, B. F. *Polymer* **2006**, *47*, 3674−3680.
(61) Milkova, V.; Radeva, T. *J. Colloid Interface Sci.* **2006**, *298*, 550−555.
(62) Severin, N.; Okhapkin, I. M.; Khokhlov, A. R.; Rabe, J. P. *Nano Lett.* **2006**, *6*, 1018−1022.
(63) Pelton, R. H. *J. Colloid Interface Sci.* **1986**, *111*, 475−485.
(64) Sukhishvili, S. A.; Granick, S. *J. Chem. Phys.* **1998**, *109*, 6869−6878.
(65) Cherstvy, A. G.; Winkler, R. G. *J. Chem. Phys.* **2004**, *120*, 9394−9400.
(66) Netz, R. R.; Joanny, J. F. *Macromolecules* **1999**, *32*, 9026−9040.
(67) Kong, C. Y.; Muthukumar, M. *J. Chem. Phys.* **1998**, *109*, 1522−1527.
(68) Varoqui, R.; Johner, A.; Elaissari, A. *J. Chem. Phys.* **1991**, *94*, 6873−6878.
(69) Castelnovo, M.; Joanny, J. F. *Langmuir* **2000**, *16*, 7524−7532.
(70) Borukhov, I.; Andelman, D.; Orland, H. *J. Phys. Chem. B* **1999**, *103*, 5042−5057.
(71) Borukhov, I. *Physica A* **1998**, *249*, 315−320.
(72) Borukhov, I.; Andelman, D.; Orland, H. *Europhys. Lett.* **1995**, *32*, 499−504.
(73) Dobrynin, A. V.; Rubinstein, M. *Prog. Polym. Sci.* **2005**, *30*, 1049−1118.

Table 2. Interaction Parameters Used in Simulations

hydrophobic polymers				hydrophilic polymers	
$\epsilon_{LJ}^{P-P} = 1.5k_BT$ $r_{cut} = 2.5\sigma$				$\epsilon_{LJ}^{P-P} = 1.0k_BT$ $r_{cut} = 2^{1/6}\sigma$	
randomly charged surface		uniformly charged surface		randomly charged surface	uniformly charged surface
hydrophilic surface	hydrophobic surface	hydrophilic surface	hydrophobic surface	hydrophilic surface	hydrophilic surface
$\epsilon_{LJ}^{S-P} = 1.0k_BT$ $r_{cut} = 2^{1/6}\sigma$ $l_B = 3.0\sigma$	$\epsilon_{LJ}^{S-P} = 1.5k_BT$ $r_{cut} = 2.5\sigma$ $l_B = 3.0\sigma$	$\epsilon_{LJ}^{S-P} = 1.0k_BT$ $r_{cut} = 2^{1/6}\sigma$ $l_B = 3.0\sigma$	$\epsilon_{LJ}^{S-P} = 1.5k_BT$ $r_{cut} = 2.5\sigma$ $l_B = 3.0\sigma$	$\epsilon_{LJ}^{S-P} = 1.0k_BT$ $r_{cut} = 2^{1/6}\sigma$ $l_B = 3.0\sigma$	$\epsilon_{LJ}^{S-P} = 1.0k_BT$ $r_{cut} = 2^{1/6}\sigma$ $l_B = 3.0\sigma$

necessity to understand the mechanism of the formation of polyelectrolyte multilayers by the successive deposition of positively and negatively charged polyelectrolytes on charged surfaces. These experiments raised an important fundamental question regarding the charge inversion in the adsorbed polyelectrolyte layers that is responsible for the successful buildup of the multicomponent polymeric films.[3] A new theoretical approach to the problem of polyelectrolyte adsorption implements the concept of the strongly correlated ionic Wigner liquid to describe polymeric layers in dilute and semidilute adsorption regimes.[7,74−76] In the framework of this approach an adsorbed layer is divided into Wigner−Seitz cells surrounding each polyelectrolyte chain. The strong lateral correlations between chains lead to surface overcharging. At higher solution ionic strengths this surface overcharging can be much larger than the bare surface charge density. In these adsorption regimes the polymer surface coverage increases with increasing salt concentration, which is a direct result of the screening of the electrostatic repulsion between adsorbed chains by the salt ions. The application of the Wigner liquid approach to concentrated polymeric layer leads to much weaker surface overcharging and nonmonotonic dependence of the polymer surface coverage on salt concentration. This is in agreement with experimental observations.[73]

While the new model of polyelectrolyte adsorption was successful in providing explanation for puzzling experimental results (for a review see ref 73), there was no attempt to verify the assumptions and test the predictions of the model in computer simulations. Previous molecular simulations of charged polymers at charged surfaces studied single chain properties and the multilayer assembly process. Monte Carlo simulations of multilayer film assembly from mixtures of oppositely charged polyelectrolytes near charged spherical particles, charged cylinders, and a uniformly charged surface were performed by Messina et al.[9,77−79] These simulations have shown that additional short-range attractive interactions between polyelectrolytes and surface are necessary to successfully initiate chain adsorption. The molecular dynamics simulations were used to study the sequential deposition of polyelectrolyte chains at a charged surface[41,44,60,80] and at charged spherical particles.[42,81] In these simulations the charged substrates were periodically exposed to dilute solutions of oppositely charged polyelctrolytes. The steady-state film growth proceeds through a charge reversal of the adsorbed polymeric film, which leads to an increase in the polymer surface coverage and in the average layer thickness after completion of the first few deposition steps. Unfortunately, these simulations were limited to the relatively narrow interval of the adsorption diagram corresponding to high surface charge densities, ensuring stability of the multilayer growth process.

In this paper, we present the results of the molecular dynamics simulations of polyelectrolyte adsorption at oppositely charged surfaces from dilute polyelectrolyte solution. We study the effect of solvent quality for the polymer backbone, polymer surface affinity, and surface charge density on the polymer surface coverage, the thickness of the adsorbed layer, and polymer surface overcharging. The rest of the paper is organized as follows. The model and simulation details are described in section 2. In section 3, we present simulation results with a detailed discussion of the dependence of the polymer surface coverage, film thickness, and surface overcharging on the surface charge density for three different polymeric systems. Finally, in section 4 we summarize our results.

2. Model and Simulation Details

We have performed molecular dynamics (MD) simulations of the adsorption of polyelectrolytes at oppositely charged surfaces from dilute solutions with polymer concentration $0.01\sigma^{-3}$. Negatively charged polyelectrolytes were modeled as bead-spring chains consisting of N_p monomers of diameter σ. In our simulations we have studied weakly charged chains with the degree of polymerizations $N_p = 61$ and fraction of charged monomers $f = 1/3$ corresponding to every third monomer carrying

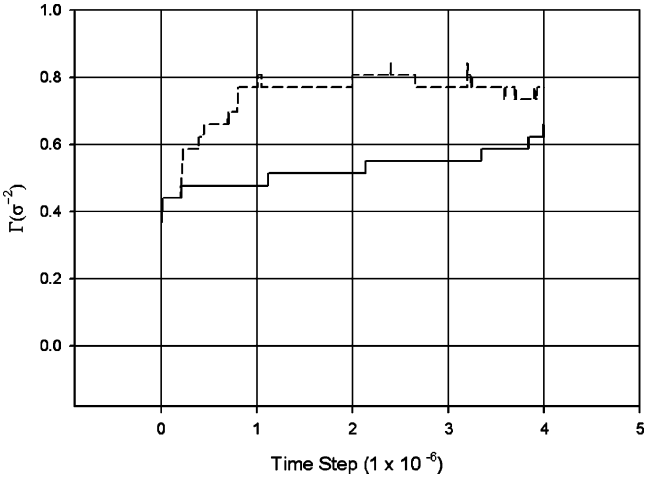

Figure 2. Evolution of the polymer surface coverage, Γ, during adsorption of hydrophilic polyelectrolytes at randomly charged hydrophobic substrate with surface charge density $\Sigma = 0.23\sigma^{-2}$. Solid line represents MD simulation without stirring steps, and dashed line corresponds to MD simulation with the stirring steps.

(74) Shklovskii, B. I. *Phys. Rev. E* **1999**, *60*, 5802−5811.
(75) Shklovskii, B. I. *Phys. Rev. Lett.* **1999**, *82*, 3268−3271.
(76) Rouzina, I.; Bloomfield, V. A. *J. Phys. Chem.* **1996**, *100*, 9977−9989.
(77) Messina, R.; Holm, C.; Kremer, K. *J. Polym. Sci., Part B: Polym. Phys.* **2004**, *42*, 3557−3570.
(78) Messina, R. *Langmuir* **2003**, *19*, 4473−4482.
(79) Messina, R. *J. Chem. Phys.* **2003**, *119*, 8133−8139.
(80) Jeon, J.; Panchagnula, V.; Pan, J.; Dobrynin, A. V. *Langmuir* **2006**, *22*, 4629−4637.
(81) Panchagnula, V.; Jeon, J.; Rusling, J. F.; Dobrynin, A. V. *Langmuir* **2005**, *21*, 1118−1125.

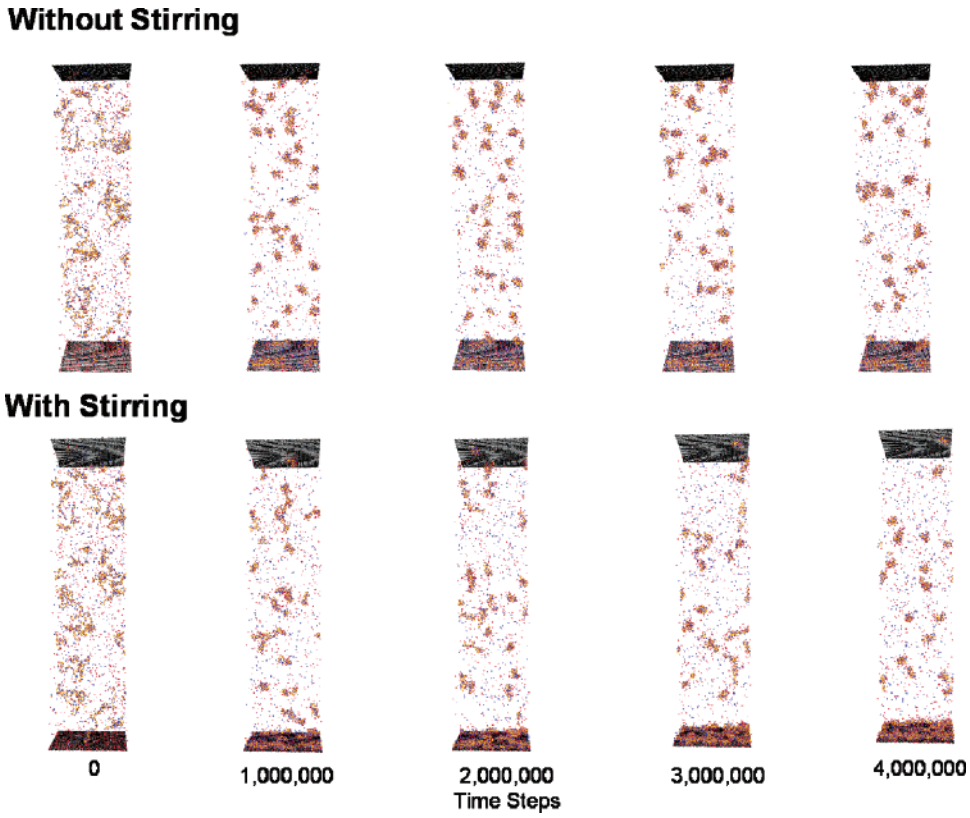

Figure 3. Evolution of the polymer and counterion distributions during the simulation runs of adsorption of hydrophobic polyelectrolytes at hydrophilic substrates.

a charge. The connectivity of beads into a chain was maintained by the finite extensible nonlinear elastic (FENE) potential.

$$U_{\mathrm{FENE}}(r) = -\frac{1}{2} k_{\mathrm{spring}} {R_{\mathrm{max}}}^2 \ln\left(1 - \frac{r^2}{{R_{\mathrm{max}}}^2}\right) \qquad (1)$$

with the spring constant $k_{\mathrm{spring}} = 30 k_{\mathrm{B}}T/\sigma^2$, where k_{B} is the Boltzmann constant and T is the absolute temperature, and the maximum bond length $R_{\mathrm{max}} = 1.5\sigma$.

Electrostatic interaction between any two charge particles with valences q_i and q_j and separated by a distance r_{ij} was given by the Coulomb potential

$$U_{\mathrm{Coul}}(r_{ij}) = k_{\mathrm{B}}T \frac{l_{\mathrm{B}} q_i q_j}{r_{ij}} \qquad (2)$$

where l_{B} is the Bjerrum length, $l_{\mathrm{B}} = e^2/\epsilon k_{\mathrm{B}}T$, defined as the length scale at which the Coulomb interaction between two elementary charges, e, in the dielectric medium of dielectric constant, ϵ, is equal to the thermal energy, $k_{\mathrm{B}}T$. In our simulations the Bjerrum length was equal to $l_{\mathrm{B}} = 3.0\sigma$. All charged monomers and counterions are monovalent ions with valence $q_i = \pm 1.0$.

The system configuration is shown in Figure 1. The positively charged adsorbing surface was modeled by a periodic hexagonal packed lattice of beads with diameter σ located at $z = 0$. A similar but uncharged nonselective surface was located at the opposite side of the simulation box to prevent chains from escaping and, hence, maintaining two-dimensional (2D) periodicity in the lateral (x and y) directions. The system size in the xy plane was equal to $40.0\sigma \times 41.6\sigma$. The height of the simulation box was varied between 161.4σ and 344.8σ to have at least twice the amount of charged monomers to compensate for the surface charges. The system sizes used in simulations are given in Table 1. We have studied polyelectrolyte adsorption at uniformly and randomly charged surfaces. In the case of uniformly charged surfaces each bead on the adsorbing surface was carrying a fractional charge with valence $q_{\mathrm{s}} = 1/2$, 2/5, 1/3, 1/4, 1/5, 1/8, and 1/16. For randomly charged surfaces charged beads were randomly distributed over the substrate and each was carrying a unit charge. We have studied systems with surface charge densities $\Sigma = 0.07\sigma^{-2}$, $0.14\sigma^{-2}$, $0.23\sigma^{-2}$, $0.29\sigma^{-2}$, $0.38\sigma^{-2}$, $0.46\sigma^{-2}$, and $0.58\sigma^{-2}$, where the surface charge density Σ is defined as the total number of charges on the surface normalized by the surface area.

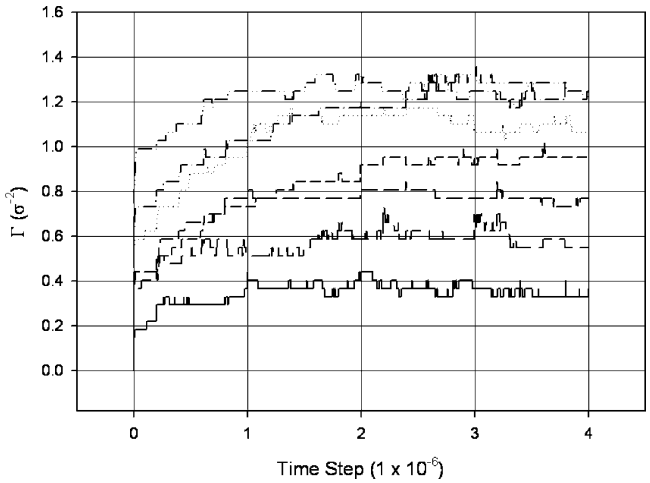

Figure 4. Evolution of the polymer surface coverage, Γ, during adsorption of hydrophilic polyelectrolytes at randomly charged hydrophilic substrate with surface charge densities: $\Sigma = 0.07\sigma^{-2}$ (solid line), $\Sigma = 0.14\sigma^{-2}$ (long dashed line), $\Sigma = 0.23\sigma^{-2}$ (intermediate dashed line), $\Sigma = 0.29\sigma^{-2}$ (short dashed line), $\Sigma = 0.38\sigma^{-2}$ (dotted line), $\Sigma = 0.46\sigma^{-2}$ (dashed dotted line), and $\Sigma = 0.58\sigma^{-2}$ (dashed double dotted line). For all surface charge densities, the stirring step was performed every 2×10^5 MD steps.

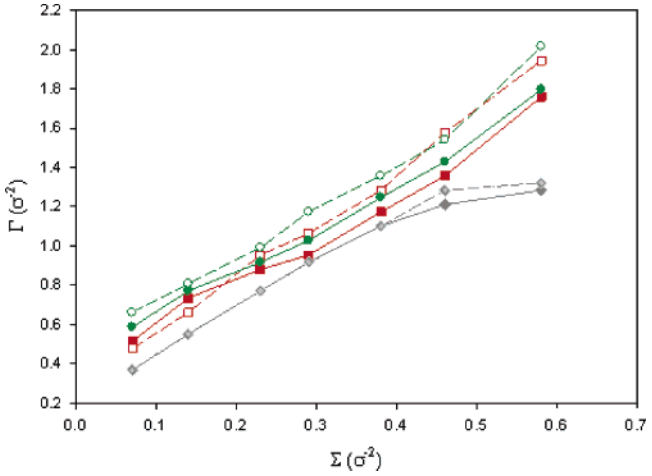

Figure 5. Dependence of the polymer surface coverage on the surface charge density for the systems of hydrophobic polyelectrolytes at hydrophilic uniformly charged surface (filled squares), hydrophobic polyelectrolytes at hydrophilic randomly charged surface (filled circles), hydrophilic polyelectrolytes at hydrophilic randomly charged surface (filled rhombus), hydrophobic polyelectrolytes at hydrophobic uniformly charged surface (open squares), hydrophobic polyelectrolytes at hydrophobic randomly charged surface (open circles), and hydrophilic polyelectrolytes at hydrophilic uniformly charged surface (rhombus with crosshair).

The particle−particle particle−mesh (PPPM) method for the slab geometry implemented in LAMMPS[82] with the sixth-order charge interpolation scheme was used to calculate the electrostatic interactions in the system. In this method, the 2D periodic images of the system are periodically replicated along the *z*-direction with distance $L = 3L_z$ between their boundaries. This reduces the problem of calculation of the electrostatic interactions in a 2D periodic system to those in a 3D system.

In addition to electrostatic interactions, all particles in a system interact through truncated-shifted Lennard-Jones (LJ) potential.

$$U_{LJ}(r_{ij}) = \begin{cases} 4\epsilon_{LJ}\left[\left(\frac{\sigma}{r_{ij}}\right)^{12} - \left(\frac{\sigma}{r_{ij}}\right)^{6} - \left(\frac{\sigma}{r_{cut}}\right)^{12} + \left(\frac{\sigma}{r_{cut}}\right)^{6}\right] & r \le r_{cut} \\ 0 & r > r_{cut} \end{cases} \quad (3)$$

The polymer−counterion, counterion−counterion, and surface−counterion LJ interaction parameters are the same and have cutoff distance $r_{cut} = 2^{1/6}\sigma$, and value of the interaction parameter $\epsilon_{LJ} = 1.0k_BT$. This choice of parameters corresponds to pure repulsive short-range interactions. The interaction parameters for the polymer−polymer and polymer−surface interactions are listed in Table 2.The simulations were carried out in a constant number of particles, volume, and temperature (*NVT*) ensemble.[83,84] The constant temperature was maintained by coupling the system to a Langevin thermostat. In this case, the equation of motion for the *i*th bead is

$$m\frac{d\vec{v}_i}{dt}(t) = \vec{F}_i(t) - \xi\vec{v}_i(t) + \vec{F}_i^R(t) \quad (4)$$

where $\vec{v}_i$ is the bead velocity and $\vec{F}_i$ is the net deterministic force acting on the *i*th bead of mass *m*. $\vec{F}_i^R$ is the stochastic force with zero average value and δ-functional correlations $\langle\vec{F}_i^R(t)\,\vec{F}_i^R(t')\rangle = 6\xi k_BT\delta(t - t')$. The friction coefficient was set to $\xi = m/\tau_{LJ}$ where τ_{LJ} is the standard LJ time, $\tau_{LJ} = \sigma(m/\epsilon_{LJ})^{1/2}$, and *m* is the particle mass that was equal to 1. The velocity Verlet algorithm was used to integrate the equations of motion.

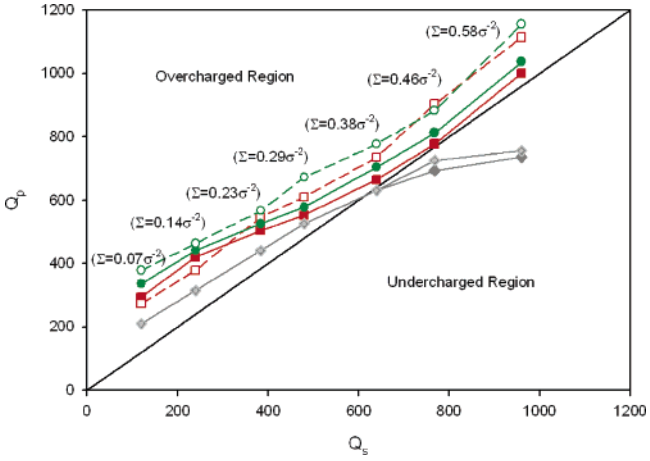

Figure 6. Dependence of the absolute value of the net charge of the adsorbed polyelectrolytes, Q_p, on the total surface charge, Q_s. Notations for the data points are the same as those in Figure 5.

The simulations were performed using the following procedure. First, *M* negatively charged polyelectrolyte chains in a self-avoiding walk configuration were randomly distributed over the simulation box. Then counterions from the charged surface and $M[(N_p - 1)/3) + 1]$ polyelectrolyte counterions were uniformly distributed over the simulation box. The initial system configuration was relaxed for 1000 MD steps with integration step $\Delta t = 0.005\tau_{LJ}$ which followed by the simulation run with the integration step $\Delta t = 0.01\tau_{LJ}$. Each simulation run continued for 4.3×10^6 MD steps.

The adsorption of polyelectrolytes at an oppositely charged surface is a two-step process. At the initial step of the adsorption process, the polymer surface coverage Γ, defined as the number density of adsorbed monomers per unit area (see Figure 2), increases very rapidly. This fast increase in the polymer surface coverage is driven by a long-range electrostatic attraction between adsorbing substrate and oppositely charged polyelectrolytes. The fast chain adsorption creates a polymer starvation zone in the vicinity of the surface (see Figure 3). At this stage the surface counterions compensate or overcompensate the remaining surface charge. This occurs because of the faster diffusion of counterions toward the surface in comparison with the diffusion of polyelectrolyte chains. The further increase of the polymer surface coverage occurs at much slower pace. This is the second step of the chain adsorption process. During this step those remaining in the simulation box polyelectrolytes have to first diffuse toward the surface and then have to overcome the electrostatic potential barrier created by adsorbed polyelectrolyte chains and counterions (see Figure 3). In order to adsorb, a polyelectrolyte has to displace already adsorbed counterions. The counterion substitution is a cooperative process, which requires lateral rearrangement of the already adsorbed polyelectrolyte chains. The incremental increase of the polymer surface coverage seen in Figure 2 at the latter stages of the adsorption process corresponds to a single chain adsorption event.

In order to speed up the adsorption process, we have performed MD simulations with stirring steps. In these simulations we have uniformly redistributed the remaining unadsorbed polyelectrolyte chains and counterions in the simulation box every 2×10^5 MD steps. Such redistribution forced chains to refill the depletion zone. The stirring process was very efficient in increasing the

(82) Plimpton, S. *LAMMPS User's Manual*; Sandia National Laboratories: Albuquerque, NM, 2005.
(83) Rapaport, D. C. *The Art of Molecular Dynamics Simulation*; Cambridge University Press: New York, 1995.
(84) Frenkel, D.; Smit, B. *Understanding Molecular Simulations*; Academic Press: San Diego, CA, 2001.

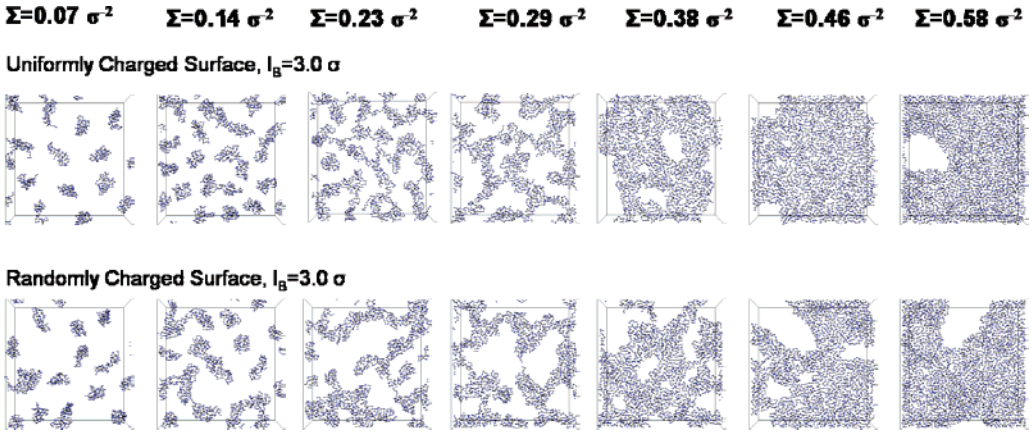

Figure 7. Snapshots of the adsorbed layer of hydrophobic polyelectrolytes at hydrophilic substrate at different surface charge densities.

polymer surface coverage at the initial stages, as shown in Figure 2, when the diffusion of the chains toward the surface was a limiting step for the chain adsorption at low surface charge densities. However, it becomes less efficient as polymer surface coverage approaches the surface neutralization and overcharging limit. At this stage of the chain adsorption process the counterion displacement and tunneling of the chain through the electrostatic potential barrier become the limiting step for the new chain adsorption.

The simulation data presented below correspond to MD simulations with stirring steps. Figure 4 shows the evolution of the polymer surface coverage during the simulation run of adsorption of hydrophilic polyelectrolytes at hydrophilic randomly charged surfaces. All plots show saturation of the polymer surface coverage at the later stages of the adsorption process, which is accompanied by adsorption and desorption events (see Figure 4). This indicates that the system reaches an equilibrium. After completion of 4.0×10^6 MD steps, we stop the stirring steps and used the final 3.0×10^5 MD steps for the data analysis. Each simulation was repeated three times to improve the data statistics.

3. Results and Discussions

Solvent quality for the polymer backbone plays an important role in determining the conformation of polyelectrolytes in solutions (see ref 73 for review). In good or θ-solvent for the polymer backbone, the chain size is estimated from the balance of the chain elasticity and electrostatic repulsion between ionized groups. The situation is qualitatively different for polyelectrolytes in a poor solvent. The shape of these polymers is determined by the interplay between electrostatic and polymer−solvent interactions. (Note that in our simulations it is the interplay between the electrostatic and monomer−monomer interactions that in fact represent an effective attraction between monomeric units in simulations without explicit solvent.) Polyelectrolyte chains in poor solvent conditions adopt a necklace-like structure of dense beads connected by strings of monomers as a compromise between electrostatic and surface energies. Large polymeric globules break up into smaller ones with increasing fraction of charged monomers on the polymer backbone. The necklace-like structure manifests itself in the unique scaling laws qualitatively different from those observed in polyelectrolyte solutions with good or θ-solvent quality for the polymer backbone (see ref 73 for review).

Additional polymer surface interactions add yet another degree of complexity in the determining factors, which control conformations of polyelectrolyte chains at oppositely charged surfaces with different affinity to the polymer backbone. Below we will show how polymer−surface affinity and surface charge density could influence the structure of the adsorbed layer.

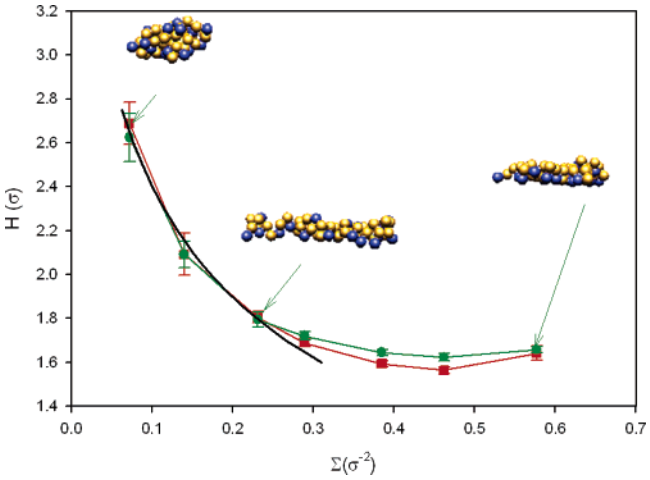

Figure 8. Dependence of the thickness of the adsorbed layer of hydrophobic polyelectrolytes at hydrophilic substrate on surface charge density. Key: randomly charged surface (filled circles) and uniformly charged surface (filled squares). Solid line is the best fit to the equation $\Sigma = 1.05(1/H^2 - 0.12/\sigma^{3/2}H^{1/2})$.

Figure 5 shows the dependence of the polymer surface coverage on the surface charge density. The polymer surface coverage for different polymeric systems shows almost linear variations with the surface charge density. However, at higher surface charge densities the polymer surface coverage for the system of hydrophilic polymers at hydrophilic surface shows saturation. In this range of the surface charge densities the polymers form a 3D adsorbed layer (see discussion below). Additional monomer−monomer short-range repulsive interactions existing between adsorbed hydrophilic polyelectrolytes hinder polymer adsorption. The value of the polymer surface coverage is the highest for the systems with the attractive short-range polymer−polymer and polymer−surface interactions (hydrophobic polyelectrolytes at hydrophobic surfaces). This is another manifestation of the importance of the short-range interactions for polyelectrolyte adsorption. The strong effect of the charge distribution on the polymer surface coverage is only observed for adsorption of hydrophobic polyelectrolytes at hydrophobic surfaces at low surface charge densities, $\Sigma < 0.23\sigma^{-2}$. With increasing surface charge density, the effect of the charge distribution diminishes.

Surface overcharging by adsorbed polyelectrolytes occurs at all surface charge densities (see Figure 6) except for systems of hydrophilic polymers adsorbing at hydrophilic surfaces with surface charge densities above $0.38\sigma^{-2}$. There is always a

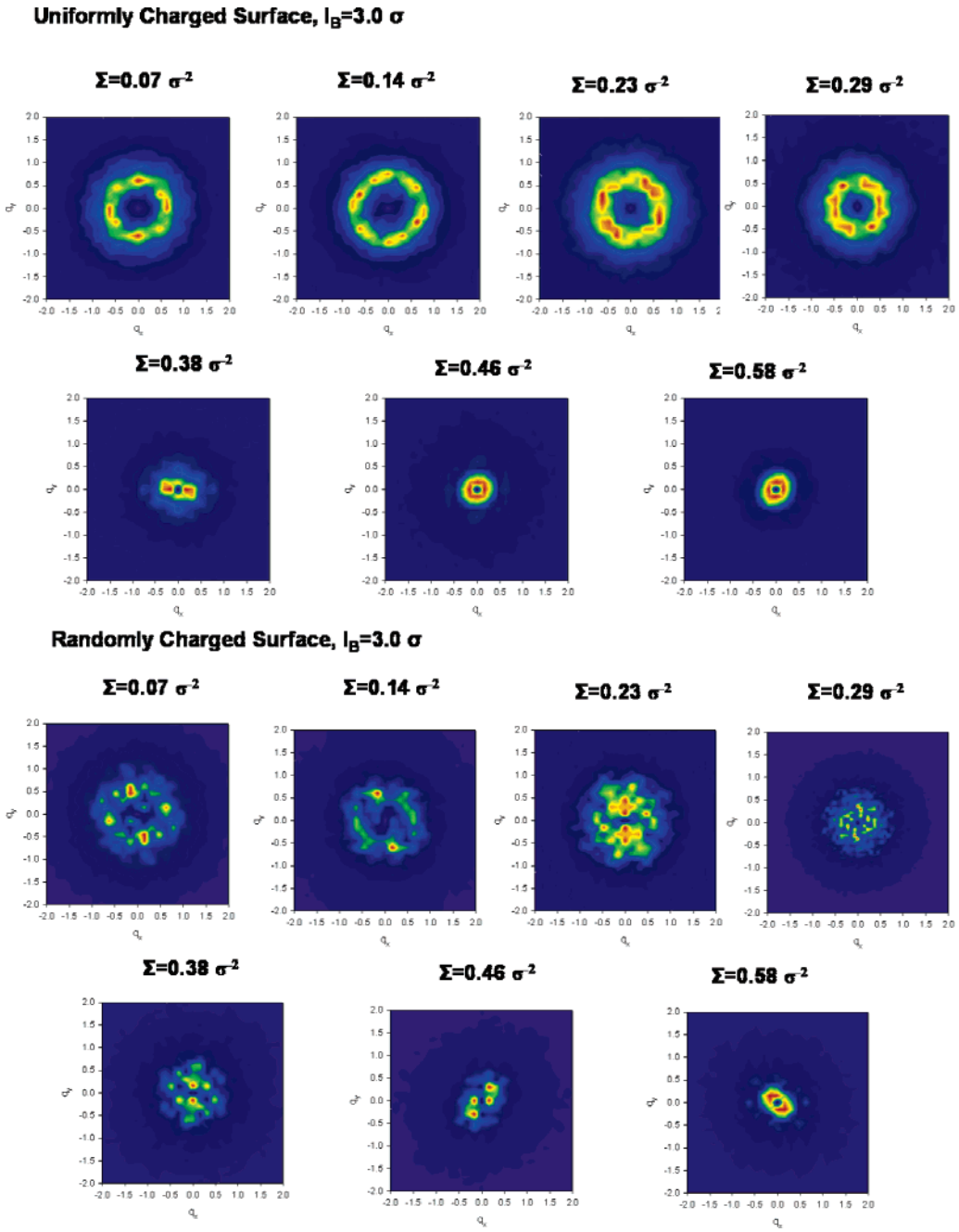

Figure 9. Evolution of the intensity plots of the monomer−monomer correlation function, $S(\mathbf{q})$, with surface charge density for the systems of hydrophobic polyelectrolyte at hydrophilic substrate.

competition between polymer chains and counterions for the available surface charge. With increasing surface charge density, the entropic penalty for counterion localization near the surface decreases. This leads to a larger number of counterions contributing to compensation of the surface charge, leaving less surface charge available for polyelectrolytes, which is manifested in a gradual decrease of the surface overcharging by polyelectrolytes with increasing surface charge density. The surface overcharging is largest for the hydrophobic randomly charged surface with surface charge density $\Sigma = 0.07\sigma^{-2}$.

The short-range interactions between polymers and substrate and solvent quality for the polymer backbone have a profound effect on the distribution of polymer density within adsorbed layer as well as on the layer thickness. Below we separately consider three qualitatively different cases.

Hydrophobic Polyelectrolytes at Hydrophilic Surfaces. This case corresponds to adsorption of hydrophobic polyelectrolytes at oppositely charged surfaces with pure repulsive LJ interactions between monomers and surface beads. At low surface charge densities $\Sigma = 0.07\sigma^{-2}$ and $\Sigma = 0.14\sigma^{-2}$ conformation of the adsorbed polyelectrolyte chain is the deformed globule (see Figure 7). The shape of the globule is slightly perturbed by the additional electrostatic attraction between negatively charged monomers and positively charged beads on the surface. The deformation of the chain increases with increasing the surface charge density. This can be seen in Figure 8 that shows the dependence of the chain thickness on the surface charge density, Σ. The deformation of a globular polyelectrolyte chain is a result of optimization of the electrostatic attraction between charged monomers and oppositely charged particles on the adsorbing surface and surface energy of the globular interface (see Appendix A). The thickness of the adsorbed layer first monotonically decreases with increasing the surface charge density and then saturates when polymer chains form a monolayer on the surface. The layer thickness dependence

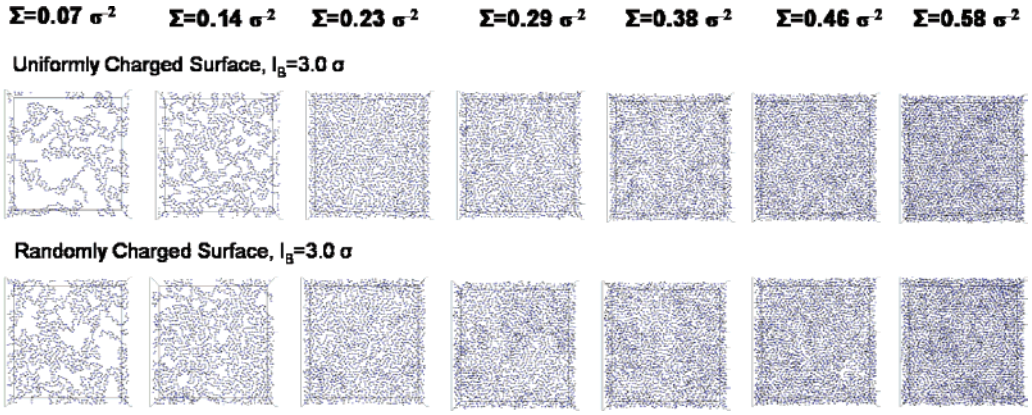

Figure 10. Snapshots of the adsorbed layer of hydrophobic polyelectrolytes at hydrophobic substrate at different surface charge densities.

on the surface charge density is in qualitative agreement with the simple scaling calculations presented in Appendix A.

The aggregation of adsorbed polyelectrolyte chains begins at surface charge density $\Sigma = 0.14\sigma^{-2}$. At this surface charge density individual globules aggregate forming elongated cylindrical globules (cylindrical domains) (see Figure 7). The driving force for this aggregation is the minimization of the surface energy of the adsorbed molecules. However, the decrease in the surface energy comes with increase in the electrostatic repulsion between charged monomers within an aggregate. Since the electrostatic interactions are exponentially screened at the length scales of the order of the Debye screening length r_D, the additional electrostatic repulsion between aggregated chains only exists within distance r_D from their boundary. The chain aggregation becomes thermodynamically favorable when the gain of the surface energy is larger than the increase in the electrostatic repulsion energy. In our simulations the Debye screening length depends on the surface charge density Σ. Adsorbed polyelectrolytes compensate for the surface charge by releasing the surface counterions, which results in approximately $2\Sigma S$ "salt" ions in the simulation box. The Debye screening length corresponding to these ions is equal to

$$r_D = (8\pi l_B \Sigma / L_z)^{-1/2} \quad (5)$$

As the surface charge density increases (the effective Debye radius decreases) more complicated domain structures start to appear (see Figure 7). In our simulations the Debye radius has varied between 7.96σ and 1.92σ. The chains start to aggregate when the value of the Debye radius becomes comparable with the *xy*-dimension of a chain. In this case the electrostatic repulsion between chains forming an aggregate is exponentially weakened by salt ions.

To analyze the domain structures we have calculated a two-dimensional Fourier transform of the monomer−monomer correlation function $S(\mathbf{q})$

$$S(\mathbf{q}) = \langle \Gamma(\mathbf{q})\Gamma(-\mathbf{q}) \rangle \quad (6)$$

where brackets correspond to an ensemble average over all distributions of the polymer density within an adsorbed layer. We have used the fast Fourier transform (FFT) method to calculate function $S(\mathbf{q})$. In order to utilize the FFT procedure, the distribution of the monomer density on the substrate $\Gamma(x,y)$ was meshed over 128×128 grid points. The meshing was implemented by the linear interpolation scheme with 2D periodic boundary conditions for the boundary grid points of the array. This procedure provides a discrete representation of the function $\Gamma(x,y)$ on the 128×128 grid points. The calculation of the 2D FFT of the function $\Gamma(x,y)$ was performed for each realization of the function $\Gamma(x,y)$ collected during the simulation run. The resultant function $S(\mathbf{q})$ was obtained by averaging the product of function $\Gamma(\mathbf{q})$ and its complex conjugated $\Gamma(\mathbf{q})^*$ over all realizations of the monomer density distribution obtained during the production run.

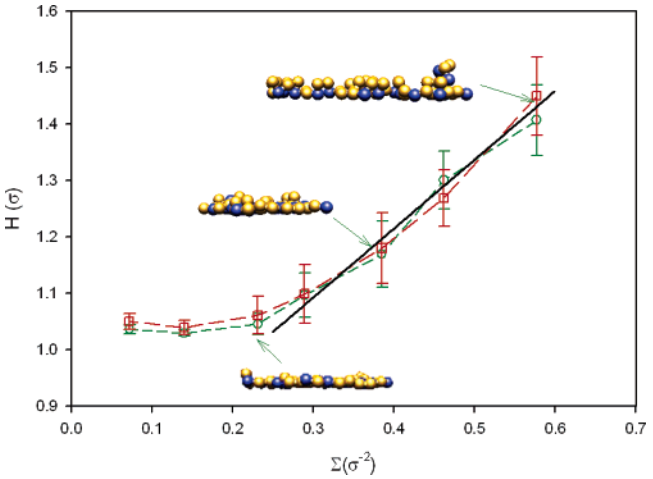

Figure 11. Dependence of the thickness of the adsorbed layer of hydrophobic polyelectrolytes at hydrophobic substrate on surface charge density. Key: randomly charged surface (open circles) and uniformly charged surface (open squares). The solid line is given by the equation $H = \sigma(0.73\Sigma\sigma^2 + 1.22)$.

Figure 9 shows evolution of the monomer−monomer correlation function $S(\mathbf{q})$ with the surface charge density Σ for uniformly and randomly charge surfaces. In the case of the uniformly charged surface, the high-intensity ring of the function $S(\mathbf{q})$ is almost isotropic. However, in the case of the random charge distribution there are high-intensity spots indicating preferential orientation of the adsorbed chains, which correlates with the substrate charge distribution. The radius q^* of the high-intensity ring decreases with increasing the surface charge density. This is in agreement with the growth of the polymer-rich regions seen in Figure 7.

Hydrophobic Polyelectrolytes at Hydrophobic Surfaces. The strong affinity between polymer backbone and adsorbing surface forces polyelectrolyte chains to spread over the surfaces forming a monolayer (see Figure 10). The flattened out polyelectrolyte chains represent an example of a 2D polyelectrolyte solution whose concentration is controlled by the electrostatic attraction between polymers and substrate. Two-dimensional hydrophobic polyelectrolyte chains already formed multichain aggregates at the lowest surface charge density $\Sigma = 0.07\sigma^{-2}$. In the case of the randomly charged surface, a high percentage of the substrate is covered with polyelectrolyte chains.

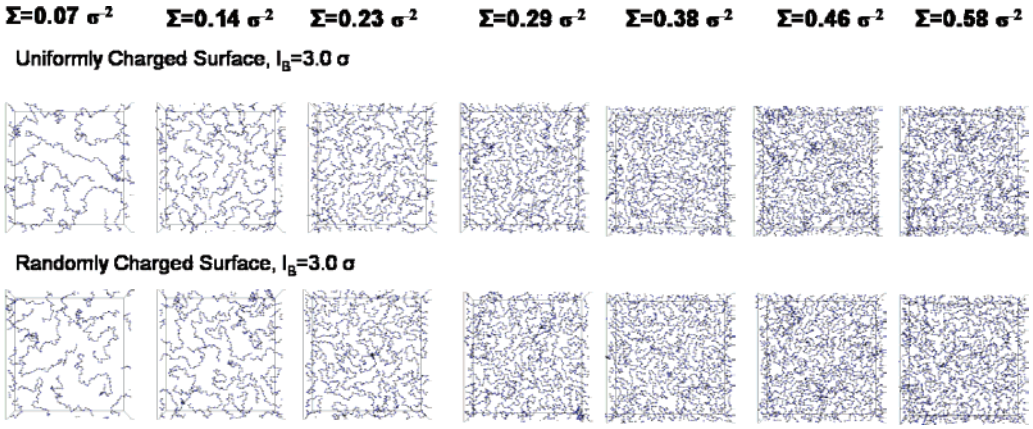

Figure 12. Snapshots of the adsorbed layer of hydrophilic polyelectrolytes at hydrophilic substrate at different surface charge densities.

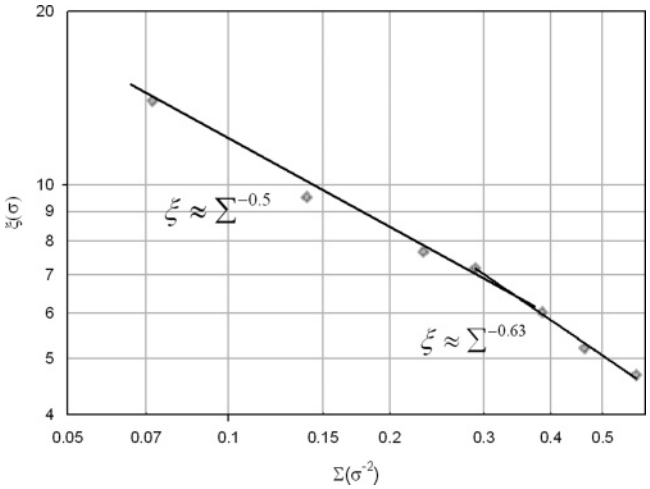

Figure 13. Dependence of the correlation blob size, ξ, on surface charge density Σ.

This is in agreement with the trend seen in Figure 5 for the dependence of the polymer surface coverage on the surface charge density. The adsorbed polyelectrolytes completely cover the surface at the surface charge density $\Sigma = 0.23\sigma^{-2}$. For higher surface charge densities, the adsorbed polyelectrolytes start to create the second and the third polymeric layers. The dependence of the average layer thickness H on the surface charge density Σ supports this fact. In the interval of the surface charge densities $\Sigma > 0.23\sigma^{-2}$ the thickness of the adsorbed layer increases linearly with the surface charge density Σ (see Figure 11). The linear increase of the layer thickness is a manifestation of the constant polymer density ρ inside the dense polymeric layer. For constant polymer density the thickness of the adsorbed layer can be estimated from the polymer surface coverage Γ as, $H \sim \Gamma/\rho$. In our case the polymer surface coverage is proportional to the surface charge density Σ (see Figure 5). (Note that the linear relationship between the surface charge density and the polymer surface coverage can also be obtained form the surface neutralization condition, $\Gamma \sim \Sigma/f$.) Thus, the layer thickness in this regime is proportional to the surface charge density, $H \sim \Sigma/\rho$ (see Figure 11). This behavior is qualitatively different from one observed for hydrophobic polyelectrolytes at hydrophilic surfaces for which the thickness of polymeric layer decreases with increasing surface charge density Σ (see Figure 8).

Hydrophilic Polyelectrolytes on Hydrophilic Surfaces. The structure of the adsorbed layer formed by the hydrophilic polyelectrolytes at hydrophilic surfaces is qualitatively different from two cases described above (see Figure 12). Hydrophilic polyelectrolyte chains form a 2D semidilute solution with the correlation length ξ, which is inversely proportional to the square root of the surface charge density[23,73]

$$\xi \sim \Sigma^{-1/2} \tag{7}$$

This scaling relation is a result of the dense packing arrangement of the correlation blobs on the adsorbing substrate. At length scales smaller than the correlation length ξ, chains are stretched by the intrachain electrostatic repulsion, while at the distances larger than the correlation length, intrachain electrostatic interactions are screened and chains follow Gaussian statistics. In the good solvent conditions for the polymer backbone the correlation blob size ξ is related to the number of monomers in it g_ξ as

$$\xi \approx \sigma(l_B f^2)^{2/7} g_\xi \tag{8}$$

The neutralization condition of the substrate by adsorbed chains leads to a requirement $fg_\xi/\xi^2 \sim \Sigma$, which can be reduced to eq 7 by using the eq 8 for the number of monomers in the correlation blob g_ξ .

To evaluate the solution correlation length, ξ, we used the scaling relation of the mean-square average end-to-end distance in the xy-plane, $\langle R_{xy}^2(m)\rangle$, of the section of the chain on the number of monomers in it m. At the length scales smaller than the solution correlation length ξ, $\langle R_{xy}^2(m)\rangle$ is proportional to m^2. At the length scales larger than the solution correlation length ξ, the electrostatic interactions are screened and $\langle R_{xy}^2(m)\rangle$ scales linearly with the number of monomers, m. The crossover value of the chain section size between two regimes corresponds to the correlation length ξ, while the crossover value for m is proportional to the number of monomers g_ξ within the correlation length ξ.

Figure 13 shows the dependence of the correlation length, ξ, on the surface charge density Σ. There are two different scaling regimes. At the low surface charge densities the correlation length ξ is indeed inversely proportional to the square root of the surface charged density Σ, $\xi \sim \Sigma^{-1/2}$. However, at higher surface charge densities, $\Sigma > 0.23\sigma^{-2}$, the correlation length decreases faster with the surface charge density. The crossover to the new scaling regime coincides with the upturn in the surface charge density dependence of the layer thickness, which marks a crossover from 2D to 3D structure of the adsorbed layer.[18,23,73]

Polyelectrolyte chains form trains and loops on the surface with charged monomers located closer to the substrate. The thickness of the adsorbed layer first decreases with increase surface charge density Σ (see Figure 14). The decrease of the layer thickness is a result of optimization of the chain confinement free energy and electrostatic attraction of the charged monomers

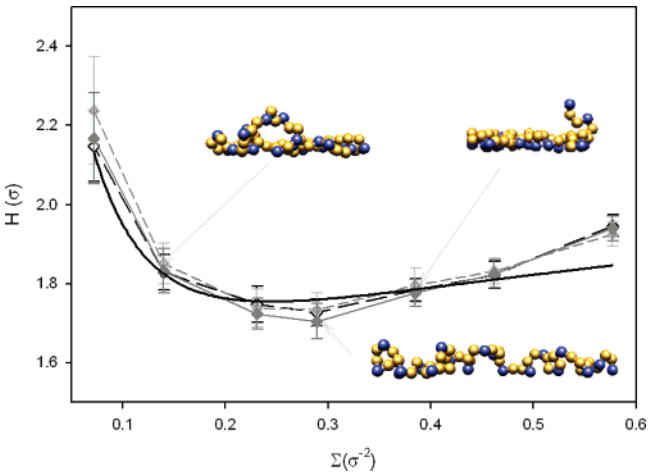

Figure 14. Dependence of the thickness of the adsorbed layer of hydrophilic polyelectrolytes at hydrophilic substrate on the surface charge density: filled rhombus, randomly charged surface, $N_p = 61$; filled rhombus with crossbars, uniformly charged surface, $N_p = 61$; open rhombus, randomly charged surface, $N_p = 43$. Solid line is given by the equation $H = \sigma(0.606(0.652/(\sum\sigma^2))^{15/8} + 22.14((\sum\sigma^2)/0.652)^{5/9})^{1/5}$.

to the oppositely charged surface. Each charged monomer on the polymer backbone is attracted to the oppositely charged background within the correlation length ξ.[18,23,73] The energy of electrostatic attraction of a charge located at distance H ($H \ll \xi$) from adsorbing surface is equal to

$$\frac{\epsilon_{ads}(H)}{k_B T} \approx -2\pi l_B \Sigma \int_0^{\xi} \frac{r\,dr}{(r^2 + H^2)^{1/2}} \approx -2\pi l_B \Sigma\, \xi\left(1 - \frac{H}{\xi}\right) \tag{9}$$

In good solvent conditions for the polymer backbone, the confinement free energy of a section of the chain with g_ξ monomers within a thickness H is equal to

$$F_{conf} \approx k_B T g_\xi \left(\frac{\sigma}{H}\right)^{5/3} \tag{10}$$

Optimization of the sum of the electrostatic attraction of fg_ξ charges and confinement free energy of the chain section with g_ξ monomers

$$\frac{F(H)}{k_B T} \approx g_\xi \left(\frac{\sigma}{H}\right)^{5/3} + 2\pi l_B g_\xi f \Sigma H \tag{11}$$

with respect to the chain thickness H results in the following expression for the layer thickness

$$H \approx \sigma(l_B \sigma f \Sigma)^{-3/8} \tag{12}$$

The thickness of the adsorbed chain (layer thickness) is independent of the degree of polymerization and decreases with the surface charge density Σ as $\Sigma^{-3/8}$.[31]

The thickness of the adsorbed layer starts to grow at the surface charge density $\Sigma = 0.23\sigma^{-2}$. This corresponds to a crossover to a 3D polymeric layer. For higher surface charge densities the thickness of the adsorbed layer is controlled by electrostatic attraction to the adsorbing surface and monomer−monomer two-body repulsive interactions. The distribution of the polymer density in this regime is obtained by solving the system of the self-consistent equations coupling distribution of the electrostatic potential and polymer density within the layer.[18,23,73] The thickness of the adsorbed layer scales with the surface charge density as

$$H \approx \sigma^{11/9} l_B^{-4/9} f^{-1} \Sigma^{1/9} \tag{13}$$

The thickness of the adsorbed layer has very weak dependence on the surface charge density Σ. This is in agreement with a slow increase of the film thickness at higher surface charge densities seen in Figure 14. To test the prediction of the scaling model, we fit our simulation data to the crossover equation

$$H \approx \left(A\left(\frac{\Sigma^*}{\Sigma}\right)^{15/8} + B\left(\frac{\Sigma}{\Sigma^*}\right)^{5/9}\right)^{1/5} \tag{14}$$

where A, B, and Σ^* are fitting parameters. This function is shown as solid line in Figure 14. The simulation data deviate from the crossover equation for the largest value of the surface charge density. It is also interesting to point out that the thickness of the adsorbed layer does not depend on the chain degree of polymerization N_p. To verify this fact, we have performed simulations of the systems with shorter chains $N_p = 43$. As one can see from Figure 14, the data points for both systems overlap.

4. Conclusions

We have performed molecular dynamics simulations of adsorption of polyelectrolytes at oppositely charged surfaces from dilute polyelectrolyte solutions. The polymer surface coverage and surface overcharging shows strong dependence on the short-range polymer−polymer and polymer−surface interactions (see Figures 5 and 6). The solvent quality for the polymer backbone and polymer affinity to the surface manifests itself in qualitatively different dependences of the thickness of the adsorbed layer on the surface charge density. In the case of adsorption of hydrophobic polyelectrolytes at hydrophilic surfaces, the chain thickness decreases with increasing surface charge density (see Figure 8). This decrease in the chain thickness is a result of the optimization of the electrostatic attraction between ionized groups on the polymer backbone to the oppositely charged substrate and beads' surface energy. Furthermore, these polyelectrolytes form multichain aggregates with increasing surface charge density.

Hydrophobic polyelectrolytes completely wet the hydrophobic surface forming a monolayer (see Figure 11). The thin polymeric layer appears as a result of maximization of the number of favorable polymer−surface contacts (see Figure 10). The thickness of the adsorbed layer stays almost constant at low surface charge densities and is mainly controlled by the strength of the short-range polymer surface interactions. However, at high surface charge densities polymers completely cover the surface and the thickness of the adsorbed layer increases linearly with the surface charge density. The linear increase of layer thickness is a result of formation of a multilayered polymeric film (see Figures 11). In this range of the surface charge densities the electrostatic attraction between polyelectrolyte chains and the oppositely charged substrate start to play a dominant role in controlling layer thickness.

Adsorption of hydrophilic polymers at hydrophilic surfaces was accompanied by nonmonotonic dependence of the chain thickness on the surface charge density shown in Figure 14. This nonmonotonicity is a result of the two different mechanisms responsible for the chain thickness stabilization. At low surface charge densities the chain thickness is determined by the balance of the energy gain due to electrostatic attraction and confinement entropy loss due to chain localization. In this regime the chain thickness decreases with increasing the surface charge density Σ. At higher surface charge densities the thickness of the adsorbed layer is determined by the balance between electrostatic attraction of the charged monomers to the substrate and short-range

monomer−monomer repulsion. This results in an increase in the layer thickness. The results of our simulations are in qualitative agreement with the prediction of the scaling models of polyelectrolyte adsorption.[18,23,31,32,73]

In many experimental situations, such as adsorption of polyelectrolyte chains from water onto clay, polymer latex particles or at the water/air interface, the dielectric constant of the solvent ϵ is larger than that of the surface ϵ_1. The presence of the charge in the medium with dielectric constant ϵ near the surface with the dielectric constant ϵ_1 causes polarization of both media. The result is the appearance of the image charge at the symmetric positions with respect to the dielectric boundary.[85] If the dielectric constant of the substrate is much smaller than the dielectric constant of the solvent $\epsilon_1 \ll \epsilon$, which is usually the case for the adsorption of polyelectrolytes from aqueous solution onto polymeric substrates, the magnitude of the image charge q' is almost equal to the valence of charge. This leads to the effective repulsion of the test charge from the dielectric boundary. Monte Carlo simulations of the effect of the dielectric boundary on the adsorption of strongly charged polyelectrolytes at oppositely charged planar surface were performed by Messina.[43] These simulations have shown that image forces appearing due to the dielectric discontinuity at the adsorbing substrate lead to the decrease in polymer surface coverage which could preclude the surface overcharging by adsorbed polyelectrolytes. We will consider the effect of the dielectric boundary on the structure of the adsorbed layer in future publications.

Acknowledgment. The authors are grateful to the donors of the Petroleum Research Fund, administered by the American Chemical Society, for support of this research under the Grant PRF#44861-AC7.

Appendix

In the case of the adsorption of the hydrophobic polyelectrolytes at hydrophilic surfaces, the dependence of the chain thickness on the surface charge density can be obtained by minimizing the free energy of the adsorbed globule

$$F_{\text{Glob}} \approx F_{\text{surf}} + F_{\text{elect}} \tag{A.1}$$

where the first term describes the surface energy of the globule with the interfacial energy γ

$$F_{\text{surf}} \approx \gamma(2\pi RH + 2\pi R^2) \tag{A.2}$$

In writing the surface energy of the globule in eq A.2, we have assumed that the globule has shape of a barrel with thickness H and radius R. The electrostatic attraction of a globule to the oppositely charged surface can be estimated as the energy of the electrostatic attraction between a charged disk of radius $R_{\text{cell}} \approx (fN_p/(\pi\Sigma))^{1/2}$ (Wigner−Seitz cell size) and a charge with valence fN_p whose center of mass is located at a distance $H/2$ from a surface which is equal to (see refs 18, 23, and 73 for details)

$$\frac{F_{\text{elect}}}{k_BT} \approx -2\pi^{1/2} l_B \Sigma^{1/2} (fN_p)^{3/2} + \pi l_B \Sigma f N_p H \tag{A.3}$$

The optimization of the surface and electrostatic energies of the globule should be done at constant globular volume, which is determined by the strength of the short-rage interactions. For the dense globule, its volume is proportional to $N_p\sigma^3 = \pi R^2 H$. Optimization of the globule free energy with respect to its thickness H leads to the following equation

$$\frac{\gamma\sigma^2}{k_BT}\left(\frac{(\pi N_p)^{1/2}}{(H\sigma)^{1/2}} - \frac{2N_p\sigma}{H^2}\right) + \pi l_B \Sigma f N_p \approx 0 \tag{A.4}$$

Without electrostatic interactions, $f = 0$, this equation has a solution $H \sim N_p^{1/3}$ and the radius of the barrel R is of the order of its thickness H. However, when there is an electrostatic attraction between a globule and a surface, the size of the deformed globule is given by

$$H \approx \sigma\left(\frac{2\tilde{\epsilon}}{\pi l_B f \Sigma\sigma}\right)^{1/2} \tag{A.5}$$

where we introduced $\tilde{\epsilon} \approx \gamma\sigma^2/(k_BT)$, the energy of a monomer on the globular surface in terms of the thermal energy k_BT. Thus, the thickness of the adsorbed globule decreases with increasing the surface charge density Σ as, $\Sigma^{-1/2}$. An adsorbed polyelectrolyte chain form a monolayer, $H \sim \sigma$, when the surface charge density Σ becomes of the order of

$$\Sigma_{\text{mon}} \approx \frac{2\tilde{\epsilon}}{\pi l_B f \sigma} \tag{A.6}$$

LA063079F

(85) Landau, L. D.; Lifshitz, E. M. *Electrodynamics of Continuous Media*, 2 ed.; Addison-Wesley: Reading, MA, 1984.